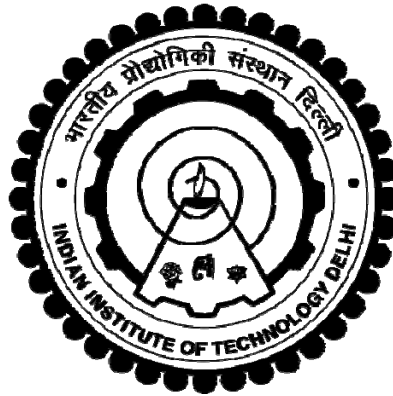


**DESIGN, MODELING AND IMPLEMENTATION OF  
IMPROVED POWER QUALITY SWITCHED MODE  
POWER SUPPLIES FOR ARC WELDING  
APPLICATIONS**

**SWATI NARULA**



**DEPARTMENT OF ELECTRICAL ENGINEERING  
INDIAN INSTITUTE OF TECHNOLOGY DELHI  
HAUZ KHAS, NEW DELHI – 110016, INDIA  
DECEMBER, 2015**

©Indian Institute of Technology Delhi (IITD), New Delhi, 2015

**DESIGN, MODELING AND IMPLEMENTATION OF  
IMPROVED POWER QUALITY SWITCHED MODE  
POWER SUPPLIES FOR ARC WELDING  
APPLICATIONS**

by

**SWATI NARULA**

**Department of Electrical Engineering**

**Submitted**

**in fulfillment of the requirements of the degree of**

**Doctor of Philosophy**

**to the**



**INDIAN INSTITUTE OF TECHNOLOGY DELHI**

**DECEMBER, 2015**

# CERTIFICATE

This is to certify that the thesis entitled “**Design, Modeling and Implementation of Improved Power Quality Switched Mode Power Supplies for Arc Welding Applications,**” being submitted by **Ms. Swati Narula** for the award of the degree of **Doctor of Philosophy** is a record of a bonafide research work carried out by her in the **Department of Electrical Engineering of Indian Institute of Technology Delhi**.

**Ms. Swati Narula** worked under our guidance and supervision and has fulfilled the requirements for the submission of this thesis, which to our knowledge has reached the requisite standard. The results obtained herein have not been submitted to any other University or Institute for the award of any degree.

**(Dr. G. Bhuvaneswari)**

Professor  
Department of Electrical Engineering  
Indian Institute of Technology Delhi  
Hauz Khas, New Delhi–110016, India.

**(Dr. Bhim Singh)**

Professor  
Department of Electrical Engineering  
Indian Institute of Technology Delhi  
Hauz Khas, New Delhi–110016, India.

**Dated:**

**New Delhi**

## ACKNOWLEDGEMENTS

I express my deepest gratitude and indebtedness to **Prof. G. Bhuvaneswari** and **Prof. Bhim Singh** for providing me the lifetime opportunity to do Ph.D work under their supervision. Working under them, has been a wonderful experience, which has provided me a deep insight into the world of research. Their sagacity and vision have played a vital role in guiding me throughout the research. Continuous monitoring, useful discussions, valuable guidance and time management by them was an inspiring force for me to complete this work. From time to time, they encouraged me for excelling in my work and it is their quest for excellence that has actuated me to improve my work and constantly introspect myself.

My sincere gratitude is reserved for all the SRC members **Prof. Sukumar Mishra**, **Prof. T.S. Bhatti** and **Dr. N. Senroy** who have been a part of the evaluating team of experts, providing me their valuable insights, suggestions and encouragement throughout my research work. My sincere thanks to **Prof. Bhim Singh**, **Prof. G. Bhuvaneswari**, **Prof. B.P. Singh**, **Prof. S.S. Murthy**, **Prof. M.L. Kothari** and **Prof. Sukumar Mishra** for their valuable inputs during my course work which helped me to enrich my knowledge.

I am grateful IIT Delhi for providing me the research facilities. Thanks are due to **Mr. Gurucharan Singh**, **Mr. Amit Kumar**, **Mr. Satey Singh Negi**, **Mr. Srichand**, **Mr. Puran Singh** and **Mr. Jagbir Singh**, lab. staff of Power Electronics and PG Machines labs. For their sustained help and co-operation rendered to carry out my dissertation work.

I extend my special thanks to the fellow research scholars **Mr. B. Amarendra Reddy**, **Mr. E. Vargil Kumar**, **Mr. T. Chandrasekhar**, **Md. Junaid**, **Mr. Raghavendra**, **Ms. Geeta Pathak**, **Ms. Yashi Singh**, **Ms. Nupur Saxena**, **Mr. Chinmay Jain**, **Mr. Ikhlq Bohru**, **Mr. Rajan Kumar Sonkar**, **Mr. Rahul Pandey** and **Mr. Aniket Anand**. My sincere thanks are due to **Dr. Shikha Singh**, **Dr. Anmol Ratan Saxena**, **Dr. R. Kalpana**, **Dr. Sandeep Madishetti**, **Dr. Vashist Bist**, **Dr. N.K. Swami Naidu**, **Dr. Sabharaj Arya**, **Dr. M. Rajesh**, **Dr. Ashish Srivastava**, **Dr. V. Rajogopal** and **Dr. Shailendra Sharma** who have given me immense moral support and shown exemplary attitude and dedication for research.

Words cannot express the feeling and gratitude I have for my father **Mr. S.P. Narula** and mother **Mrs. Ranju Narula** for their constant encouragement, support and personal sacrifices they made to push me forward to allow me to reach new levels of excellence. I thank my sisters

for their support and love that allowed me to complete my PhD work. Once again, I bow to all those who directly or indirectly helped me but whose names are left out.

Last but not the least I'm beholden to almighty for their blessings to help me to raise my academic level to this stage. I pray for their benediction in my future endeavors. May their blessings be showered on me for strength, wisdom and determination to achieve in future goals also!

(Swati Narula)

## ABSTRACT

In the process of achieving increased energy efficiency, power density and reliability, switch mode power supplies (SMPSs) have become an accepted part of the electronic systems. SMPSs are now standard equipment for the majority of our industrial and home appliances due to their ruggedness, efficacy, low cost, compactness and reliability. As a result of their performance, SMPSs are widely used in the most applications to provide an efficient and effective source of power. Moreover, with recent advances in semiconductors, magnetic and passive technologies make the SMPS an ever more popular choice in many electronic equipments such as for computers, LEDs, net-books, chargers, motor drives, telecommunication tower power supplies, military equipment, aerospace applications etc. and the demand is ever-increasing. Most of these power supplies utilize AC-DC converters at the front end that are either diode bridge or phase controlled rectifiers. Although these SMPSs are highly efficient, due to their non-linear behavior they draw highly distorted current resulting in low power factor (PF) and high total harmonic distortion (THD). This deterioration in power quality (PQ) leads to increased system losses, degrading the shelf-life of electrical equipments, high electromagnetic interference, etc. With the all pervasive nature of these SMPSs, distribution systems face escalated PQ issues which affect the other equipment in the electrical systems. The proliferation of SMPS in industrial applications has accentuated the PQ issues faced by utilities and consumers making the research on improved PQ utility interface come to the forefront and to look for a possible opportunity to mitigate the associated PQ problems. The increasing awareness about PQ and adverse effects of harmonics pollution have persuaded the power supply manufacturers to maintain THD and PF within the permissible levels which are imposed by international standards, such as IEEE-519 and IEC-61000. In fact, these standards have enforced a constraint on the new electronic devices coming up these days in terms of maintaining a reasonable input PQ. Therefore, an emphasis is laid on the development of simple, economical and energy efficient SMPSs having high PF, low CF and reduced input current harmonics. Certainly, cost, size, design simplicity etc. are amongst the challenging constraints to deal with the goal to mitigate the input PQ issues.

Arc welding is amongst the widely used and efficient welding processes in many industries. However, arc welding power supplies (AWPSs) are considered as a potential source of harmonics. This work is an endeavour to develop an AWPS with improved power factor and less

current harmonic content at the utility interface. The AWPSs that are currently available in the market are devoid of power factor correction and input PQ improvement. An enhancement in the performance of AWPSs is required to achieve good process controllability, portability, improved efficiency and better PQ. Simplicity has always been one of the main features of medium and high capacity SMPSs. This constrains them to use a diode bridge rectifier (DBR) followed by a bulky DC link capacitor at the front end. The second stage usually comprises an isolated DC-DC converter. However, this type of conventional SMPS draws a highly distorted, harmonic rich, peaky input current having a poor PF at the AC mains leading to deterioration of the system performance. With significant variations in the load, it draws a highly non-sinusoidal input current at low PF resulting in a poor converter operation. This research work presents different methods of improving the PQ at the point of common coupling (PCC) for single-phase and three-phase AC mains fed AWPSs. It provides a thorough analysis of the converters and investigates to provide suitable utility interfaces for both types of AWPSs. As a result, with concise analysis and design approach, high performance improved PQ AWPSs with stiffly regulated output voltage along with overcurrent handling capability have been designed, simulated and developed in single-phase and three-phase configurations.

Various single-stage and two-stage PFC-converters which have been classified into DBR based, bridgeless, interleaved, multilevel, modular and multipulse converter configurations for single-phase and three-phase systems have been designed, modeled and implemented in hardware to improve the PQ at the PCC. The single-stage SMPSs are preferred because of their advantages like high power density, simple control, high efficiency, reduced size and load sharing capability. However, two-stage power supplies are ideal for higher power ratings and enhanced control on output parameters. Besides, the control strategy of the PFC converters also plays a vital role in deciding the overall performance, complexity, cost and size of SMPS. In this work, most of the PFC converters have been designed to operate in discontinuous conduction mode (DCM), however, PFC converters of higher power rating function in continuous conduction mode (CCM). Ultimately, the output voltage and output current of the power supply are regulated depending on the loading conditions. Pulse width modulation (PWM) technique has been utilized for the switching of high frequency switches used in PFC converters. During the arc welding process, the load variations happen very rapidly over a wide range. This causes several problems such as spattering, poor weld bead quality, instability of arc length, etc. So, it is

expected of a good AWPS to work efficiently during light load as well as overload conditions. AWPS stands out as a special entity as compared to other power supplies because over-current limiting capability is mandatory for welding applications. The performances of the PFC converters in the AWPS are evaluated during their steady state operation, load variation and short circuit at the output terminals.

Several non-isolated and isolated DBR based as well as bridgeless converter configurations have been investigated to mitigate the PQ issues associated with AWPSs. Bridgeless converter configurations have been realized to minimize the conduction losses of the converter and to improve thermal utilization. These DBR based and bridgeless converters have been designed, modeled and implemented in hardware to verify their performance during various operating conditions. Further, interleaved converters have been explored to increase the power rating of the SMPS and to reduce the input current ripple. By interleaving the PFC converters, the input current is bifurcated into two or more, therefore devices of reduced rating can be utilized. Hardware results also have been presented to validate the advantages of interleaving technique.

In the case of three-phase AWPSs, multilevel, multipulse and modular converter configurations are presented. For the multi-level case, three-level converter has been used at the front end for PFC and isolated DC-DC converter has been used at the rear end for voltage scaling. The overall configuration ensures that the output voltage remains constant and output current is limited during the overload conditions. The simulated performances have also been verified experimentally on the developed prototype. In any power electronic circuit, lower order harmonics are dominant and form the majority of the harmonic content present in the AC mains current. An 18-pulse AC-DC converter configuration, that would eliminate until 17th harmonic, has been explored and analyzed for arc welding applications. With an increase in the pulse number, the cost and complexity of the overall system also increases. An 18-pulse converter turns out to be optimal because of fairly manageable level of complexity despite eliminating most of the lower order harmonics. Hence, an 18-pulse converter based AWPS has been designed, modeled and implemented to validate its viability and proficiency. The modular configuration utilizes single-phase modules to form three-phase power supply. The aim of this configuration is to make the SMPS robust and flexible in terms of maintenance and power expandability. Various isolated DC-DC converter configurations have been designed, modeled and simulated to reduce the input current THD and to achieve unity PF at the input AC mains.

The major contribution of this thesis is two-fold: (i) input PQ improvement by using PFC converters in single-phase and three-phase configurations and (ii) voltage regulation and over current limit at the output end. Therefore, AWPSs having improved PQ with output voltage and current regulation have been designed, modeled and implemented using single-stage and two-stage PFC converters for single-phase and three-phase systems. The performance of the power supply has been investigated over wide range of loads. A substantial improvement in PQ indices has been achieved under varying loads apart from regulating the output voltage stiffly and limiting the current appreciably even under short circuit conditions.

# TABLE OF CONTENTS

	<b>Page No.</b>
Certificate	i
Acknowledgements	iii
Abstract	v
Table of Contents	ix
List of Figures	xxv
List of Tables	xliii
List of Abbreviations/Symbols	xlv

## **CHAPTER I INTRODUCTION**

1.1	General	1
1.2	State of Art on SMPS for Arc Welding Applications	3
1.3	Power Quality Standards	6
1.4	Scope of Work	7
1.4.1	Analysis, Design and Development of Single Phase PFC-SMPS with Improved Power Quality	8
1.4.2	Analysis, Design and Development of a Single Phase Bridgeless PFC-SMPS with Improved Power Quality	9
1.4.3	Analysis, Design and Development of a Three Phase Three Level PFC-SMPS with Improved Power Quality	9
1.4.4	Analysis, Design and Development of a Three Phase Multi-Pulse PFC-SMPS with Improved Power Quality	9
1.4.5	Analysis, Design and Development of Three Phase Modular PFC-SMPS with Improved Power Quality	10
1.5	Outlines of Chapters	10

## **CHAPTER II LITERATURE REVIEW**

2.1	General	13
2.2	Significant Developments in SMPS	14
2.3	Literature Survey	14
2.3.1	Single-Stage SMPS for Arc Welding	16
2.3.1.1	Single-stage SMPSs using isolated converter	17
2.3.1.2	Single-stage SMPSs using isolated bridgeless converter	18

2.3.1.3	Single-stage SMPSs using modular converter	18
2.3.2	Two-Stage SMPS for Arc Welding	19
2.3.2.1	Two-stage SMPS using bridgeless PFC converter	20
2.3.2.2	Two-stage SMPS using interleaved PFC converter	22
2.3.2.3	Two-stage SMPS using multipulse PFC converter	23
2.3.2.4	Two-stage SMPS using multilevel PFC converter	23
2.4	Identified Research Areas	24
2.5	Conclusions	25

### **CHAPTER III CLASSIFICATION AND CONFIGURATION OF SINGLE PHASE AND THREE PHASE SMPS FOR ARC WELDING**

3.1	General	27
3.2	Requirement of PFC-SMPS for Arc Welding	28
3.3	Classification of SMPS for Arc Welding	29
3.3.1	Classification of Single-Stage SMPS for Arc Welding	30
3.3.2	Classification of Two-Stage SMPS for Arc Welding	31
3.3.3	Classification of Bridgeless AC-DC Converter Based SMPS for Arc Welding	31
3.3.4	Classification of Interleaved AC-DC Converter Based SMPS for Arc Welding	31
3.3.5	Classification of Multi-level AC-DC Converter Based SMPS for Arc Welding	31
3.3.6	Classification of Multi-pulse AC-DC Converter Based SMPS for Arc Welding	32
3.3.7	Classification of Modular AC-DC Converter Based SMPS for Arc Welding	32
3.4	Configurations of Single-Phase and Three-Phase SMPS for Arc Welding	32
3.4.1	Configurations of Single-Phase Single-Stage SMPS for Arc Welding	32
3.4.1.1	Configurations of single-phase single-stage AC-DC converter based SMPS	33
3.4.1.2	Configurations of single-phase single-stage bridgeless AC-DC converter based SMPS	33
3.4.2	Configurations of Single-Phase Two-Stage SMPS for Arc Welding	36
3.4.2.1	Configurations of single-phase two-stage AC-DC converter based SMPS	36
3.4.2.2	Configurations of single-phase two-stage interleaved AC-DC converter based SMPS	40
3.4.2.3	Configurations of single-phase two-stage bridgeless AC-DC converter based SMPS	42

3.4.3	Configurations of Three-Phase Single-Stage SMPS for Arc Welding	45
3.4.3.1	Configurations of three-phase single-stage modular AC DC converter based SMPS	46
3.4.3.2	Configurations of three-phase single-stage bridgeless modular AC-DC converter based SMPS	48
3.4.4	Configurations of Three-Phase Two-Stage SMPS for Arc Welding	49
3.4.4.1	Configurations of three-phase two-stage multi-pulse AC-DC converter based SMPS	50
3.4.4.2	Configurations of three-phase two-stage multi-level AC DC converter based SMPS	50
3.5	Hardware Implementation of SMPS for Arc Welding	52
3.5.1	Development of Isolation and Amplification Circuit for PWM Signals	52
3.5.2	Development of Signal Conditioning Circuit for Voltage and Current Sensors	53
3.6	Conclusions	55

**CHAPTER IV DESIGN, MODELING AND IMPLEMENTATION OF SINGLE-PHASE SINGLE STAGE IMPROVED POWER QUALITY SMPS FOR ARC WELDING**

4.1	General	57
4.2	Circuit Configurations of Single Phase Single Stage Improved Power Quality AWPS	58
4.2.1	Circuit Configuration of a Two-Switch Isolated Zeta Converter Based AWPS	58
4.2.2	Circuit Configuration of an Isolated Sheppard-Taylor Based AWPS	59
4.3	Modes of Operation of Single Phase Single Stage Improved Power Quality AWPS	59
4.3.1	Modes of Operation of Two-Switch Isolated Zeta Converter Based AWPS	60
4.3.2	Modes of Operation of Sheppard Taylor Converter Based AWPS	62
4.4	Design of Single Phase Single Stage Improved Power Quality AWPS	62
4.4.1	Design of Two-Switch Isolated Zeta Converter Based AWPS	62
4.4.2	Design of Sheppard Taylor Converter Based AWPS	65
4.5	Control of Single Phase Single Stage Improved Power Quality AWPS	67
4.5.1	Control of Two-Switch Isolated Zeta Converter Based AWPS	68
4.5.2	Control of Sheppard Taylor Converter Based AWPS	69
4.6	MATLAB Modeling of Single Phase Single Stage Improved Power Quality AWPS	70
4.6.1	MATLAB Modeling of Two-Switch Isolated Zeta Converter Based AWPS	70
4.6.2	MATLAB Modeling of Sheppard Taylor Converter Based AWPS	70

4.7	Hardware Implementation of Single Phase Single Stage Arc Welding Power Supply	71
4.8	Results and Discussion	72
4.8.1	Simulated Performance of the Single Phase Single Stage Improved Power Quality AWPS	72
4.8.1.1	Performance of two-switch isolated zeta converter based AWPS	73
4.8.1.1.1	Performance at rated load condition	73
4.8.1.1.2	Performance under light load condition	74
4.8.1.1.3	Performance under overload condition	75
4.8.1.2	Performance of Sheppard Taylorconverter based AWPS	75
4.8.1.2.1	Performance at rated load condition	76
4.8.1.2.2	Performance under light load condition	76
4.8.1.2.3	Performance under overload condition	77
4.8.2	Experimental Performance of the Single Phase Single Stage Improved Power Quality AWPS	78
4.8.2.1	Performance at rated load condition	79
4.8.2.2	Performance under light load condition	81
4.8.2.3	Performance under overload condition	82
4.9	Conclusions	83

**CHAPTER V DESIGN, MODELING AND IMPLEMENTATION OF SINGLE PHASE SINGLE STAGE IMPROVED POWER QUALITY BRIDGELESS CONVERTER BASED SMPS FOR ARC WELDING**

5.1	General	85
5.2	Circuit Configurations of Single Phase Single Stage Improved Power Quality Bridgeless Converter Based AWPS	86
5.2.1	Circuit Configuration of Isolated Bridgeless Full Bridge Converter Based AWPS	86
5.2.2	Circuit Configuration of Isolated Bridgeless Cuk Converter Based AWPS	88
5.2.3	Circuit Configuration of Isolated Bridgeless SEPIC Based AWPS	90
5.2.4	Circuit Configuration of Isolated Bridgeless Zeta Converter Based AWPS	91
5.3	Modes of Operation of Single Phase Single Stage Improved Power Quality Bridgeless Converter Based AWPS	93
5.3.1	Modes of Operation of Isolated Bridgeless Full Bridge Converter Based AWPS	95
5.3.2	Modes of Operation of Isolated Bridgeless Cuk Converter Based AWPS	97

5.3.3	Modes of Operation of Isolated Bridgeless SEPIC Based AWPS	99
5.3.4	Modes of Operation of Isolated Bridgeless Zeta Converter Based AWPS	101
5.4	Design of Single Phase Single Stage Improved Power Quality Bridgeless Converter Based AWPS	101
5.4.1	Design of Isolated Bridgeless Full Bridge Converter Based AWPS	103
5.4.2	Design of Isolated Bridgeless Cuk Converter Based AWPS	104
5.4.3	Design of Isolated Bridgeless SEPIC Based AWPS	107
5.4.4	Design of Isolated Bridgeless Zeta Converter Based AWPS	110
5.5	Control of Single Phase Single Stage Improved Power Quality Bridgeless Converter Based AWPS	112
5.6	MATLAB Modeling of Single Phase Single Stage Improved Power Quality Bridgeless Converter Based AWPS	112
5.6.1	MATLAB Modeling of Isolated Bridgeless Full Bridge Converter Based AWPS	113
5.6.2	MATLAB Modeling of Isolated Bridgeless Cuk Converter Based AWPS	114
5.6.3	MATLAB Modeling of Isolated Bridgeless SEPIC Based AWPS	114
5.6.4	MATLAB Modeling of Isolated Bridgeless Zeta Converter Based AWPS	115
5.7	Hardware Implementation of Single Phase Single Stage Improved Power Quality Bridgeless Converter Based AWPS	116
5.8	Results and Discussion	117
5.8.1	Simulated Performance of the Single Phase Single Stage Improved Power Quality AWPS	117
5.8.1.1	Performance of isolated bridgeless full bridge converter based AWPS	117
5.8.1.1.1	Performance at rated load condition	118
5.8.1.1.2	Performance under light load condition	119
5.8.1.1.3	Performance under overload condition	120
5.8.1.2	Performance of isolated bridgeless Cuk converter based AWPS	120
5.8.1.2.1	Performance at rated load condition	120
5.8.1.2.2	Performance under light load condition	122
5.8.1.2.3	Performance under overload condition	122
5.8.1.3	Performance of isolated bridgeless SEPIC based AWPS	123
5.8.1.3.1	Performance at rated load condition	123
5.8.1.3.2	Performance under light load condition	125
5.8.1.3.3	Performance under overload condition	126
5.8.1.4	Performance of isolated bridgeless zeta converter based AWPS	126

	5.8.1.4.1	Performance at rated load condition	127
	5.8.1.4.2	Performance under light load condition	128
	5.8.1.4.3	Performance under overload condition	128
5.8.2	Experimental Performance of the Single Phase Single Stage Improved Power Quality AWPS		130
5.9	Conclusions		132

**CHAPTER VI DESIGN, MODELING AND IMPLEMENTATION OF SINGLE PHASE TWO STAGE IMPROVED POWER QUALITY BOOST CONVERTER BASED SMPS FOR ARC WELDING**

6.1	General		135
6.2	Circuit Configurations of Single Phase Two Stage Improved Power Quality Boost Converter Based AWPS		136
	6.2.1	Circuit Configuration of Boost Converter Based AWPS	137
	6.2.2	Circuit Configuration of Interleaved Boost Converter Based AWPS	137
	6.2.3	Circuit Configuration of Bridgeless Boost Converter Based AWPS	139
6.3	Modes of Operation of Single Phase Two Stage Improved Power Quality Boost Converter Based AWPS		140
	6.3.1	Modes of Operation of Boost Converter Based AWPS	140
		6.3.1.1 Operating modes of boost converter	141
		6.3.1.2 Operating modes of isolated FB buck converter	142
	6.3.2	Modes of Operation of Interleaved Boost Converter Based AWPS	142
	6.3.3	Modes of Operation of Bridgeless Boost Converter Based AWPS	147
6.4	Design of Single Phase Two Stage Improved Power Quality Boost Converter Based AWPS		149
	6.4.1	Design of Boost Converter Based AWPS	150
		6.4.1.1 Design of boost converter	150
		6.4.1.2 Design of isolated FB buck converter	152
	6.4.2	Design of Interleaved Boost Converter Based AWPS	153
	6.4.3	Design of Bridgeless Boost Converter Based AWPS	153
6.5	Control of Single Phase Two Stage Improved Power Quality Boost Converter Based AWPS		154
	6.5.1	Control of Boost Converter	155
	6.5.2	Control of Isolated FB Buck Converter	156
6.6	MATLAB Modeling of Single Phase Two Stage Improved Power Quality Boost Converter Based AWPS		157
	6.6.1	MATLAB Modelling of Boost Converter Based AWPS	157

6.6.2	MATLAB Modelling of Interleaved Boost Converter Based AWPS	157
6.6.3	MATLAB Modelling of Bridgeless Boost Converter Based AWPS	159
6.7	Hardware Implementation of Single Phase Two Stage Improved Power Quality Boost Converter Based AWPS	159
6.7.1	Hardware Implementation of Boost Converter Based AWPS	160
6.7.2	Hardware Implementation of Interleaved Boost Converter Based AWPS	160
6.7.3	Hardware Implementation of Bridgeless Boost Converter Based AWPS	160
6.8	Results and Discussion	161
6.8.1	Performance of Conventional AWPS	162
6.8.2	Simulated Performance of the Single Phase Two Stage Improved Power Quality Boost Converter Based AWPS	162
6.8.2.1	Performance of boost converter based AWPS	162
6.8.2.1.1	Performance at rated load condition	163
6.8.2.1.2	Performance under light load condition	163
6.8.2.1.3	Performance under overload condition	164
6.8.2.2	Performance of interleaved boost converter based AWPS	165
6.8.2.2.1	Performance at rated load condition	165
6.8.2.2.2	Performance under light load condition	166
6.8.2.2.3	Performance under overload condition	167
6.8.2.3	Performance of bridgeless boost converter based AWPS	167
6.8.2.3.1	Performance at rated load condition	168
6.8.2.3.2	Performance under light load condition	168
6.8.2.3.3	Performance under overload condition	169
6.8.3	Experimental Performance of Single Phase Two Stage Improved Power Quality Boost Converter Based AWPS	170
6.8.3.1	Performance of boost converter based AWPS	170
6.8.3.1.1	Performance at rated load condition	171
6.8.3.1.2	Performance under light load condition	172
6.8.3.1.3	Performance under overload condition	173
6.8.3.2	Performance of interleaved boost converter based AWPS	174
6.8.3.2.1	Performance at rated load condition	174
6.8.3.2.2	Performance under light load condition	178
6.8.3.2.3	Performance under overload condition	178
6.8.3.3	Performance of bridgeless boost converter based AWPS	179
6.8.3.3.1	Performance at rated load condition	180

	6.8.3.3.2	Performance under light load condition	182
	6.8.3.3.3	Performance under overload condition	183
6.9		Conclusions	184

**CHAPTER VII DESIGN, MODELING AND IMPLEMENTATION OF SINGLE PHASE TWO STAGE IMPROVED POWER QUALITY BUCK-BOOST CONVERTERS BASED SMPS FOR ARC WELDING**

7.1		General	185
7.2		Circuit Configurations of Single Phase Two Stage Improved Power Quality Buck-Boost Converter Based AWPS	186
	7.2.1	Circuit Configuration of Cuk Converter Based AWPS	186
	7.2.2	Circuit Configuration of a SEPIC Based AWPS	186
	7.2.3	Circuit Configuration of a Zeta Converter Based AWPS	187
	7.2.4	Circuit Configuration of a CSC Converter Based AWPS	188
	7.2.5	Circuit Configuration of an Interleaved CSC Converter Based AWPS	189
7.3		Modes of Operation of Single Phase Two Stage Improved Power Quality Buck-Boost Converter Based AWPS	190
	7.3.1	Modes of Operation of Cuk Converter Based AWPS	191
	7.3.2	Modes of Operation of SEPIC Based AWPS	193
	7.3.3	Modes of Operation of Zeta Converter Based AWPS	194
	7.3.4	Modes of Operation of CSC Converter Based AWPS	197
	7.3.5	Modes of Operation of Interleaved CSC Converter Based AWPS	198
7.4		Design of Single Phase Two Stage Improved Power Quality Buck-Boost Converter Based AWPS	201
	7.4.1	Design of Cuk Converter Based AWPS	204
	7.4.2	Design of SEPIC Based AWPS	205
	7.4.3	Design of Zeta Converter Based AWPS	208
	7.4.4	Design of CSC Converter Based AWPS	209
	7.4.5	Design of Interleaved CSC Converter Based AWPS	211
7.5		Control of Single Phase Two Stage Improved Power Quality Buck-Boost Converter Based AWPS	212
7.6		MATLAB Modeling of Single Phase Two Stage Improved Power Quality Buck-Boost Converter Based AWPS	213
	7.6.1	MATLAB Modeling of Cuk Converter Based AWPS	213
	7.6.2	MATLAB Modeling of SEPIC Based AWPS	214
	7.6.3	MATLAB Modeling of Zeta Converter Based AWPS	214
	7.6.4	MATLAB Modeling of CSC Converter Based AWPS	215
	7.6.5	MATLAB Modeling of Interleaved CSC Converter Based AWPS	216

7.7	Hardware Implementation of Single Phase Two Stage Improved Power Quality Buck-Boost Converter Based AWPS	216
7.7.1	Hardware Implementation of CSC Converter Based AWPS	217
7.7.2	Hardware Implementation of Interleaved CSC Converter Based AWPS	218
7.8	Results and Discussion	219
7.8.1	Performance of Conventional AWPS	219
7.8.2	Simulated Performance of the Single Phase Two Stage Improved Power Quality Buck-Boost Converter Based AWPS	220
7.8.2.1	Performance of Cuk converter based AWPS	220
7.8.2.1.1	Performance at rated load condition	220
7.8.2.1.2	Performance under light load condition	220
7.8.2.1.3	Performance under overload condition	221
7.8.2.2	Performance of SEPIC based AWPS	223
7.8.2.2.1	Performance at rated load condition	223
7.8.2.2.2	Performance under light load condition	223
7.8.2.2.3	Performance under overload condition	225
7.8.2.3	Performance of Zeta Converter based AWPS	225
7.8.2.3.1	Performance at rated load condition	226
7.8.2.3.2	Performance under light load condition	226
7.8.2.3.3	Performance under overload condition	226
7.8.2.4	Performance of CSC Converter based AWPS	227
7.8.2.4.1	Performance at rated load condition	227
7.8.2.4.2	Performance under light load condition	228
7.8.2.4.3	Performance under overload condition	229
7.8.2.5	Performance of Interleaved CSC Converter based AWPS	230
7.8.2.5.1	Performance at rated load condition	231
7.8.2.5.2	Performance under light load condition	233
7.8.2.5.3	Performance under overload condition	234
7.8.3	Experimental Performance of Single Phase Two Stage Improved Power Quality Buck-Boost Converter Based AWPS	234
7.8.3.1	Performance of CSC converter based AWPS	235
7.8.3.1.1	Performance at rated load condition	235
7.8.3.1.2	Performance under light load condition	237
7.8.3.1.3	Performance under overload condition	239
7.8.3.1	Performance of Interleaved CSC converter based AWPS	240

	7.8.3.1.1	Performance at rated load condition	240
	7.8.3.1.2	Performance under light load condition	241
	7.8.3.1.3	Performance under overload condition	242
7.9		Conclusions	244

**CHAPTER VIII DESIGN, MODELING AND IMPLEMENTATION OF SINGLE PHASE TWO STAGE IMPROVED POWER QUALITY BRIDGELESS BUCK-BOOST CONVERTERS BASED SMPS FOR ARC WELDING**

8.1		General	247
8.2		Circuit Configurations of Single Phase Two Stage Improved Power Quality Bridgeless Buck-Boost Converter Based AWPS	248
	8.2.1	Circuit Configuration of Bridgeless Cuk Converter Based AWPS	248
	8.2.2	Circuit Configuration of Bridgeless SEPIC Based AWPS	251
	8.2.3	Circuit Configuration of Bridgeless Zeta Based AWPS	252
	8.2.4	Circuit Configuration of Bridgeless CSC Based AWPS	254
8.3		Modes of Operation of Single Phase Two Stage Improved Power Quality Bridgeless Buck-Boost Converter Based AWPS	255
	8.3.1	Modes of Operation of Bridgeless Cuk Converter Based AWPS	257
	8.3.2	Modes of Operation of Bridgeless SEPIC Based AWPS	258
	8.3.3	Modes of Operation of Bridgeless Zeta Converter Based AWPS	260
	8.3.4	Modes of Operation of Bridgeless CSC Converter Based AWPS	262
8.4		Design of Single Phase Two Stage Improved Power Quality Bridgeless Buck-Boost Converter Based AWPS	263
	8.4.1	Design of Bridgeless Cuk Converter Based AWPS	263
	8.4.2	Design of Bridgeless SEPIC Based AWPS	264
	8.4.3	Design of Bridgeless Zeta Converter Based AWPS	264
	8.4.4	Design of Bridgeless CSC Converter Based AWPS	265
8.5		Control of Single Phase Two Stage Improved Power Quality Bridgeless Buck-Boost Converter Based AWPS	266
8.6		MATLAB Modeling of Single Phase Two Stage Improved Power Quality Bridgeless Buck-Boost Converter Based AWPS	267
	8.5.1	MATLAB Modeling of Bridgeless Cuk Converter Based AWPS	268
	8.5.2	MATLAB Modeling of Bridgeless SEPIC Based AWPS	268
	8.5.3	MATLAB Modeling of Bridgeless Zeta Converter Based AWPS	269
	8.5.4	MATLAB Modeling of Bridgeless CSC Converter Based AWPS	270
8.7		Hardware Implementation of Single Phase Two Stage Improved Power Quality Bridgeless Buck-Boost Converter Based AWPS	271

8.6.1	Hardware Implementation of Bridgeless Zeta Converter Based AWPS	271
8.6.2	Hardware Implementation of Bridgeless CSC Converter Based AWPS	272
8.8	Results and Discussion	273
8.8.1	Performance of Conventional AWPS	273
8.8.2	Simulated Performance of Single Phase Two Stage Improved Power Quality Bridgeless Buck-Boost Converter Based AWPS	274
8.8.2.1	Performance of bridgeless Cuk converter based AWPS	274
8.8.2.1.1	Performance at rated load condition	274
8.8.2.1.2	Performance under light load condition	274
8.8.2.1.3	Performance under overload condition	275
8.8.2.2	Performance of Bridgeless SEPIC Based AWPS	277
8.8.2.2.1	Performance at rated load condition	277
8.8.2.2.2	Performance under light load condition	279
8.8.2.2.3	Performance under overload condition	279
8.8.2.3	Performance of Bridgeless Zeta Converter Based AWPS	280
8.8.2.3.1	Performance at rated load condition	280
8.8.2.3.2	Performance under light load condition	281
8.8.2.3.3	Performance under overload condition	283
8.8.2.4	Performance of Bridgeless CSC Converter Based AWPS	284
8.8.2.4.1	Performance at rated load condition	284
8.8.2.4.2	Performance under light load condition	285
8.8.2.4.3	Performance under overload condition	286
8.8.3	Experimental Performance of Single Phase Two Stage Improved Power Quality Bridgeless Buck-Boost Converter Based AWPS	286
8.8.3.1	Performance of Bridgeless Zeta Converter Based AWPS	287
8.8.3.1.1	Performance at rated load condition	287
8.8.3.1.2	Performance under light load condition	290
8.8.3.1.3	Performance under overload condition	291
8.8.3.2	Performance of Bridgeless CSC Converter Based AWPS	292
8.8.3.2.1	Performance at rated load condition	293
8.8.3.2.2	Performance under light load condition	295
8.8.3.2.3	Performance under overload condition	296
8.9	Conclusions	297

**CHAPTER IX DESIGN, MODELING AND IMPLEMENTATION OF THREE PHASE IMPROVED POWER QUALITY THREE LEVEL CONVERTER BASED SMPS FOR ARC WELDING**

9.1	General	299
9.2	Circuit Configuration of Three Phase Improved Power Quality Three Level Converter Based AWPS	300
9.3	Modes of Operation of Three Phase Improved Power Quality Three Level Converter Based AWPS	301
9.4	Design of Operation of Three Phase Improved Power Quality Three Level Converter Based AWPS	303
9.5	Control of Operation of Three Phase Improved Power Quality Three Level Converter Based AWPS	307
9.6	MATLAB Modeling of Three Phase Improved Power Quality Three Level Converter Based AWPS	309
9.7	Hardware Implementation of Three Phase Improved Power Quality Three Level Converter Based AWPS	310
9.8	Results and Discussion	311
9.8.1	Simulated Performance of Three Phase Three Level AWPS	311
9.8.1.1	Performance at rated load condition	312
9.8.1.2	Performance under light load condition	312
9.8.1.3	Performance under overload condition	313
9.8.2	Experimental Performance of Three Phase Three Level AWPS	314
9.8.2.1	Performance at rated load condition	315
9.8.2.2	Performance under light load condition	318
9.8.2.3	Performance under overload condition	319
9.9	Conclusions	320

**CHAPTER X DESIGN, MODELING AND IMPLEMENTATION OF THREE PHASE IMPROVED POWER QUALITY MULTIPULSE CONVERTER BASED SMPS FOR ARC WELDING**

10.1	General	321
10.2	Circuit Configuration of Three Phase Multipulse Converter Based AWPS	322
10.3	Design of Three Phase Multipulse Converter Based AWPS	323
10.4	Control of Three Phase Multipulse Converter Based AWPS	331
10.5	MATLAB Modeling of Three Phase Three Level Multi-Pulse AC-DC Converter Based AWPS	331
10.6	Hardware Implementation of Three Phase Three Level Multi-Pulse AC-DC Converter Based AWPS	332
10.7	Results and Discussion	333

10.7.1	Simulated Performance of Three Phase Multipulse Converter Based AWPS	333
10.7.1.1	Performance at rated condition	334
10.7.1.2	Performance under light load condition	335
10.7.1.3	Performance under overload condition	338
10.7.2	Experimental Performance of Three Phase Multipulse Converter Based AWPS	338
	Performance at rated load condition	338
	Performance under light load condition	340
	Performance under overload condition	341
10.9	Conclusions	341

**CHAPTER XI DESIGN, MODELING AND SIMULATION OF THREE PHASE SINGLE STAGE IMPROVED POWER QUALITY MODULAR CONVERTER BASED SMPS FOR ARC WELDING**

11.1	General	345
11.2	Circuit Configurations of Three Phase Single Stage Improved Power Quality Modular Converter Based AWPS	346
11.2.1	Circuit Configuration of Isolated Full Bridge Converter Based AWPS	347
11.2.2	Circuit Configuration of Isolated Push-Pull Converter Based AWPS	348
11.2.3	Circuit Configuration of Isolated Cuk Converter Based AWPS	348
11.2.4	Circuit Configuration of Isolated Zeta Converter Based AWPS	350
11.2.5	Circuit Configuration of a Bridgeless Isolated Cuk Converter Based AWPS	350
11.2.6	Circuit Configuration of a Bridgeless Isolated Zeta Converter Based AWPS	351
11.3	Modes of Operation of Three Phase Single Stage Improved Power Quality Modular Converter Based AWPS	352
11.3.1	Modes of Operation of FB Converter Based Modular AWPS	353
11.3.2	Modes of Operation of Push-Pull Converter Based Modular AWPS	355
11.4	Design of Three Phase Single Stage Improved Power Quality Modular Converter Based AWPS	356
11.5	Control of Three Phase Single Stage Improved Power Quality Modular Converter Based AWPS	361
11.6	MATLAB Modeling of Three Phase Single Stage Improved Power Quality Modular Converter Based AWPS	362
11.6.1	MATLAB Modeling of Isolated Full Bridge Modular Converter Based AWPS	363
11.6.2	MATLAB Modeling of Isolated Push-Pull Modular Converter Based AWPS	364

11.6.3	MATLAB Modeling of Isolated Cuk Modular Converter Based AWPS	364
11.6.4	MATLAB Modeling of Isolated Zeta Modular Converter Based AWPS	365
11.6.5	MATLAB Modeling of Isolated Bridgeless Cuk Modular Converter Based AWPS	366
11.6.6	MATLAB Modeling of Isolated Bridgeless Zeta Modular Converter Based AWPS	367
11.7	Results and Discussion	367
11.7.1	Performance of Isolated Full Bridge Modular Converter Based AWPS	368
11.7.1.1	Performance at rated load condition	368
11.7.1.2	Performance under light load condition	369
11.7.1.3	Performance under overload condition	370
11.7.2	Performance of Isolated Push-Pull Modular Converter Based AWPS	371
11.7.2.1	Performance at rated load condition	371
11.7.2.2	Performance under light load condition	372
11.7.2.3	Performance under overload condition	373
11.7.3	Performance of Isolated Cuk Converter Based Modular AWPS	373
11.7.3.1	Performance at rated load condition	374
11.7.3.2	Performance under light load condition	374
11.7.3.3	Performance under overload condition	375
11.7.4	Performance of Isolated Zeta Modular Converter Based AWPS	376
11.7.4.1	Performance at rated load condition	377
11.7.4.2	Performance under light load condition	378
11.7.4.3	Performance under overload condition	379
11.7.5	Performance of Isolated Bridgeless Cuk Modular Converter Based AWPS	379
11.7.5.1	Performance at rated load condition	380
11.7.5.2	Performance under light load condition	381
11.7.5.3	Performance under overload condition	381
11.7.6	Performance of Isolated Bridgeless Zeta Modular Converter Based AWPS	382
11.7.6.1	Performance at rated load condition	383
11.7.6.2	Performance under light load condition	384
11.7.6.3	Performance under overload condition	384
11.8	Conclusions	386

**CHAPTER XII MAIN CONCLUSIONS AND SUGGESTIONS FOR FURTHER WORK**

12.1	General	387
12.2	Main Conclusions	388
12.3	Suggestions for Further Work	391
	<b>REFERENCES</b>	393
	<b>APPENDICES</b>	415
	<b>LIST OF PUBLICATIONS</b>	425
	<b>BIO-DATA</b>	427

## LIST OF FIGURES

- Fig. 3.1 Classification of SMPSs for arc welding.
- Fig. 3.2 Single-phase single-stage modified isolated zeta converter based SMPS.
- Fig. 3.3 Single-phase single-stage Sheppard-Taylor converter based SMPS.
- Fig. 3.4 Single-phase single-stage BL full bridge converter based SMPS.
- Fig. 3.5 Single-phase single-stage BL-Cuk converter based SMPS.
- Fig. 3.6 Single-phase single-stage BL-SEPIC based SMPS.
- Fig. 3.7 Single-phase single-stage BL-zeta converter based SMPS.
- Fig. 3.8 Single-phase two-stage boost converter based SMPS.
- Fig. 3.9 Single-phase two-stage Cuk converter based SMPS.
- Fig. 3.10 Single-phase two-stage SEPIC based SMPS.
- Fig. 3.11 Single-phase two-stage zeta converter based SMPS.
- Fig. 3.12 Single-phase two-stage CSC converter based SMPS.
- Fig. 3.13 Schematic diagram of single-phase two-stage interleaved boost converter based SMPS.
- Fig. 3.14 Circuit configuration of single-phase two-stage interleaved CSC converter based SMPS.
- Fig. 3.15 Schematic diagram of single-phase two-stage BL-boost converter based SMPS.
- Fig. 3.16 Circuit configuration of single-phase two-stage BL Cuk converter based SMPS.
- Fig. 3.17 Circuit configuration of single-phase two-stage BL-SEPIC based SMPS.
- Fig. 3.18 Circuit configuration of the BL-zeta converter based SMPS.
- Fig. 3.19 Schematic of BL-CSC converter based SMPS.
- Fig. 3.20 Schematic of modular full bridge converter based SMPS.
- Fig. 3.21 Schematic of modular push-pull converter based SMPS.
- Fig. 3.22 Schematic of modular isolated Cuk converter based SMPS.
- Fig. 3.23 Circuit configuration of modular isolated zeta converter based SMPS.
- Fig. 3.24 Circuit configuration of BL modular Cuk converter based SMPS.
- Fig. 3.25 Circuit configuration of BL modular zeta converter based SMPS.
- Fig. 3.26 Circuit configuration of 18-pulse converter based SMPS.
- Fig. 3.27 Circuit configuration of Vienna rectifier based SMPS.
- Fig. 3.28 Schematic of isolation and amplification circuit diagram.

- Fig. 3.29 Developed hardware prototype of opto-isolation circuitry.
- Fig. 3.30 Schematic of voltage sensor LV-25P.
- Fig. 3.31 Developed hardware prototype of voltage sensor circuitry.
- Fig. 3.32 Schematic of current sensor LA-55P.
- Fig. 3.33 Developed hardware prototype of current sensor circuitry.
- Fig. 4.1 Basic configuration of single-stage SMPS.
- Fig. 4.2 TS isolated zeta converter based AWPS.
- Fig. 4.3 Circuit configuration of the proposed Sheppard-Taylor converter based AWPS.
- Fig. 4.4 Operating modes of TS isolated zeta converter based AWPS, (a) Mode I; (b) Mode II; (c) Mode III; (d) Waveforms during one switching period.
- Fig. 4.5 Operating modes of Sheppard Taylor converter based AWPS, (a) Mode I; (b) Mode II; (c) Mode III; (d) Waveforms during one switching period.
- Fig. 4.6 Control scheme for proposed TS zeta converter based SMPS.
- Fig. 4.7 Control scheme for proposed Sheppard Taylor converter based SMPS.
- Fig. 4.8 MATLAB model of SMPS using TS zeta converter.
- Fig. 4.9 MATLAB model of SMPS using Sheppard Taylor converter.
- Fig. 4.10 Photograph of the developed laboratory prototype of the single-stage TS zeta converter based AWPS.
- Fig. 4.11 Steady state performance of the TS zeta converter based AWPS.
- Fig. 4.12 Harmonic spectrum of AC mains current,  $i_s$  at rated load conditions.
- Fig. 4.13 Dynamic performance of the TS zeta converter based AWPS under light load condition.
- Fig. 4.14 Harmonic spectrum of AC mains current,  $i_s$  during light load conditions.
- Fig. 4.15 Dynamic performance of TS zeta converter based AWPS during short circuit condition.
- Fig. 4.16 Performance of the AWPS using Sheppard Taylor converter at rated load.
- Fig. 4.17 Input AC mains current ( $i_s$ ) along with its harmonic spectrum at rated load.
- Fig. 4.18 Dynamic performance of the Sheppard Taylor converter based AWPS at 20% load.
- Fig. 4.19 Waveform and harmonics spectrum of AC mains current ( $i_s$ ) at light load (20%) condition.
- Fig. 4.20 Performance of the Sheppard Taylor converter based AWPS during short circuit condition.

- Fig. 4.21 Performance of the proposed AWPS at 220 V AC mains and 100% load.
- Fig. 4.22 Inductor current ( $i_{L_o}$ ) and intermediate capacitor's voltage ( $v_{C1}$ ) at rated load condition.
- Fig. 4.23 Voltage and current stress of PFC switch at rated load condition.
- Fig. 4.24 Enlarged voltage and current stress of PFC switch at rated load condition.
- Fig. 4.25 PQ indices and performance parameters ( $v_s$ ,  $i_s$ , P, Q, S, PF, DPF, CF and THD of  $i_s$  of proposed TS zeta converter based AWPS at full load; (a) Input voltage and current; (b) Input power, PF and DPF; (c) Harmonic spectrum of input phase current,  $i_s$ .
- Fig. 4.26 Dynamic performance of the proposed AWPS at light load (20%) condition.
- Fig. 4.27 PQ indices and performance parameters ( $v_s$ ,  $i_s$ , P, Q, S, PF, DPF, CF and THD of  $i_s$  of proposed TS zeta converter based AWPS at light load condition; (a) Input voltage and current; (b) Input power, PF and DPF; (c) Harmonic spectrum of input phase current,  $i_s$ .
- Fig. 4.28 Dynamic performance of the proposed AWPS for the case of overload condition.
- Fig. 5.1 Basic configuration of single phase single-stage SMPS.
- Fig. 5.2 Isolated BL-FB converter based SMPS.
- Fig. 5.3 Operating circuits of BL-FB converter during (a) positive and (b) negative half-cycles of supply voltage.
- Fig. 5.4 Circuit configuration of isolated BL-Cuk converter based SMPS.
- Fig. 5.5 Operating circuits of isolated BL-Cuk converter during (a) positive and (b) negative half-cycles of the supply voltage.
- Fig. 5.6 Circuit configuration of isolated BL SEPIC converter based AWPS.
- Fig. 5.7 Operating circuits of isolated BL-SEPIC during (a) positive and (b) negative half-cycles of the supply voltage.
- Fig. 5.8 Circuit configuration of the isolated BL zeta converter based AWPS.
- Fig. 5.9 Operating circuits of isolated BL-zeta converter during (a) positive and (b) negative half-cycles of the supply voltage.
- Fig. 5.10 Operating modes of BL-FB converter during positive half cycle of the supply voltage for the period of one switching cycle.
- Fig. 5.11 Operating modes of isolated BL-Cuk converter during positive half cycle of the supply voltage for the period of one switching cycle.
- Fig. 5.12 Operating modes of isolated BL-SEPIC during positive half cycle of the supply voltage for the period of one switching cycle.

- Fig. 5.13 Operating modes of isolated zeta converter during positive half cycle of the supply voltage for the period of one switching cycle.
- Fig. 5.14 MATLAB model of BL-FB converter based AWPS.
- Fig. 5.15 MATLAB model of BL-Cuk converter based AWPS.
- Fig. 5.16 Schematic diagram of MATLAB model of BL-SEPIC based AWPS.
- Fig. 5.17 Schematic diagram of MATLAB model of BL-zeta converter based AWPS.
- Fig. 5.18 Experimental setup of the developed hardware of isolated BL-zeta converter based AWPS.
- Fig. 5.19 Performance of BL-FB converter based AWPS at full load.
- Fig. 5.20 Waveform of input current and its harmonic spectrum at rated load.
- Fig. 5.21 Performance of BL-FB converter based AWPS during light load condition.
- Fig. 5.22 Waveform of input current and its harmonic spectrum at light load.
- Fig. 5.23 Performance of BL-FB converter based AWPS during overload condition.
- Fig. 5.24 Performance of isolated BL-Cuk converter based AWPS at full load.
- Fig. 5.25 Waveform of input current and its harmonic spectrum at rated load.
- Fig. 5.26 Dynamic performance of isolated BL-Cuk converter based AWPS during light load condition.
- Fig. 5.27 Waveform of input current and its harmonic spectrum during light load.
- Fig. 5.28 Performance of isolated BL-Cuk converter based AWPS during overload condition.
- Fig. 5.29 Performance of isolated BL-SEPIC based AWPS at full load.
- Fig. 5.30 Waveform of input current and its harmonic spectrum at rated load.
- Fig. 5.31 Dynamic performance of isolated BL-SEPIC based AWPS during light load condition.
- Fig. 5.32 Waveform of input current and its harmonic spectrum during light load.
- Fig. 5.33 Performance of isolated BL-SEPIC based AWPS during overload condition.
- Fig. 5.34 Performance of isolated BL-zeta converter based AWPS at full load.
- Fig. 5.35 Waveform of input current and its harmonic spectrum at rated load.
- Fig. 5.36 Dynamic performance of isolated BL-zeta converter based AWPS during light load condition.
- Fig. 5.37 Waveform of input current and its harmonic spectrum during light load.
- Fig. 5.38 Performance of isolated BL-zeta converter based AWPS during extreme overload condition.

- Fig. 5.39 Input voltage, input current and output voltage and current of isolated BL-zeta converter.
- Fig. 5.40 Input voltage, intermediate capacitor voltage, output inductor current of BL-zeta converter.
- Fig. 5.41 Input voltage, switch stress of the switch conducting in positive half cycle of the input voltage.
- Fig. 5.42 PQ indices and performance parameters of the isolated BL-zeta converter based AWPS at rated load; (a) Input voltage and current; (b) Input power, PF and DPF; (c) Harmonic spectrum of input phase current,  $i_s$ .
- Fig. 5.42 PQ indices and performance parameters of the isolated BL-zeta converter based AWPS at rated load; (a) Input voltage and current; (b) Input power, PF and DPF; (c) Harmonic spectrum of input phase current,  $i_s$ .
- Fig. 6.1 Schematic of two-stage AWPS using PFC boost converter and isolated FB converter.
- Fig. 6.2 Schematic diagram of interleaved boost converter based AWPS.
- Fig. 6.3 Schematic diagram of two-stage SMPS using bridgeless boost converter and isolated FB converter.
- Fig. 6.4 Bridgeless boost converter during (a) positive and (b) negative half-cycles of the supply voltage.
- Fig. 6.5 Steady state operation of the PFC boost converter; (a) Mode I and (b) Mode II.
- Fig. 6.6 Operation of FB buck converter (a) Mode-I: switch  $S_1$  and  $S_4$  conducting, (b) Mode-II: both the switches are off, (c) Mode-III: switch  $S_2$  and  $S_3$  are on, (d) Mode-IV: both the switches are off.
- Fig. 6.7 Operation of the steady state interleaved boost converter (a) Mode-I, both the switches are on; (b) Mode-II, switch  $S_{b1}$  is on; (c) Mode-III, switch  $S_{b2}$  is on; (d) Mode-IV, both the switches are off.
- Fig. 6.8 Waveforms across different components of interleaved boost converter (a) when  $D < 0.5$  i.e.  $v_s < V_b/2$ ; (b) when  $D > 0.5$  i.e.  $v_s < V_b/2$ .
- Fig. 6.9 Operation of the steady state BL boost converter during the positive half-cycle of the supply voltage; (a) Mode I and (b) Mode II.
- Fig. 6.10 Operation of the steady state BL boost converter during the negative half-cycle of the supply voltage; (a) Mode I and (b) Mode II.
- Fig. 6.11 MATLAB model of boost converter based AWPS.
- Fig. 6.12 MATLAB model of interleaved boost converter based AWPS.
- Fig. 6.13 MATLAB model of bridgeless boost converter based AWPS.

- Fig. 6.14 Experimental setup of developed hardware of the PFC-boost converter based AWPS.
- Fig. 6.15 Photograph of developed hardware of interleaved boost converter based AWPS.
- Fig. 6.16 Photograph of developed hardware of bridgeless boost converter based AWPS.
- Fig. 6.17 Recorded PQ indices of conventional AWPS at rated load with supply voltage at 220V. (a) Conventional AWPS input voltage and current; (b) Input power and PF; (c) Harmonic spectrum of input current.
- Fig. 6.18 Performance of boost converter based AWPS at rated load condition.
- Fig. 6.19 Input current and its harmonic spectrum at 220V under rated load condition.
- Fig. 6.20 Dynamic performance of boost converter based AWPS during light load condition.
- Fig. 6.21 Input current and its harmonic spectrum at 220V under light load condition.
- Fig. 6.22 Performance of the boost converter based AWPS during overload condition.
- Fig. 6.23 Performance of the interleaved boost converter based AWPS at full load.
- Fig. 6.24 Input current and its harmonic spectrum at 220V at rated load condition.
- Fig. 6.25 Dynamic performance of interleaved boost converter based AWPS during light load condition.
- Fig. 6.26 Input current and its harmonic spectrum at 220V under light load condition.
- Fig. 6.27 Dynamic performance of the interleaved boost converter based AWPS during overload condition.
- Fig. 6.28 Performance of the bridgeless boost converter based AWPS at rated load condition.
- Fig. 6.29 Input current and its harmonic spectrum at 220V at rated load condition.
- Fig. 6.30 Performance of the bridgeless boost converter based AWPS during light load condition.
- Fig. 6.31 Waveform of input current and its harmonic spectrum during light load.
- Fig. 6.32 Dynamic performance of bridgeless boost converter based AWPS during overload condition.
- Fig. 6.33 Supply voltage, supply current and output voltage and current of FB DC-DC converter.
- Fig. 6.34 Supply voltage, supply current and output voltage and current of boost DC-DC converter.
- Fig. 6.35 Waveform of input inductor current ( $i_{Lb}$ ) demonstrating CCM operation.

- Fig. 6.36 Power quality indices and performance parameters of the PFC-boost converter based AWPS at rated load; (a) Input voltage and current; (b) Input power, PF and DPF; (c) Harmonic spectrum of input current,  $i_s$ .
- Fig. 6.37 Supply voltage, supply current and output voltage and current of FB DC-DC converter during light load condition.
- Fig. 6.38 Power quality indices and performance parameters of the boost converter based AWPS during light load; (a) Input voltage and current; (b) Input power, PF and DPF; (c) Harmonic spectrum of input current,  $i_s$ .
- Fig. 6.39 Supply voltage, supply current and output voltage and current of FB DC-DC converter during overload condition.
- Fig. 6.40 Supply voltage, supply current and output voltage and current of FB DC-DC converter.
- Fig. 6.41 Supply voltage, supply current and output voltage and current of interleaved boost converter.
- Fig. 6.42 Supply voltage, input inductor currents ( $i_{Lb1}$  and  $i_{Lb2}$ ) and  $i_{Lb}$  demonstrating interleaving technique.
- Fig. 6.43 Supply voltage, supply current, input inductor current  $i_{Lb1}$  and  $i_{Lb}$  demonstrating CCM operation.
- Fig. 6.44 Voltage stress across the switches ( $S_{b1}$  and  $S_{b2}$ ) at rated load condition when  $D < 0.5$ .
- Fig. 6.45 Voltage stress across the switches ( $S_{b1}$  and  $S_{b2}$ ) at rated load condition when  $D > 0.5$ .
- Fig. 6.46 Power quality indices and performance parameters of the interleaved boost converter based AWPS at rated load; (a) input voltage and current; (b) Input power, PF and DPF; (c) Harmonic spectrum of input current,  $i_s$ .
- Fig. 6.47 Supply voltage & current and output voltage & current of the FB DC-DC converter during light load condition.
- Fig. 6.48 Power quality indices and performance parameters of the interleaved boost converter based AWPS during light load; (a) Input voltage and current; (b) Input power, PF and DPF; (c) Harmonic spectrum of input current,  $i_s$ .
- Fig. 6.49 Input voltage, input current and output voltage and current of FB DC-DC converter during overload condition.
- Fig. 6.50 Supply voltage, supply current and output voltage and current of FB DC-DC converter.
- Fig. 6.51 Supply voltage, supply current and output voltage and current of bridgeless boost DC-DC converter.

- Fig. 6.52 Supply voltage, supply current and switch voltage stress of bridgeless boost converter.
- Fig. 6.53 Waveforms of supply voltage, supply current and boost inductor currents showing CCM operation.
- Fig. 6.54 Power quality indices and performance parameters of the bridgeless boost converter based AWPS at rated load; (a) input voltage and current; (b) Input power, PF and DPF; (c) Harmonic spectrum of input current,  $i_s$ .
- Fig. 6.55 Input voltage, input current and output voltage and current of FB DC-DC converter during light load condition.
- Fig. 6.56 Power quality indices and performance parameters of the bridgeless boost converter based AWPS during light load; (a) Input voltage and current; (b) Input power, PF and DPF; (c) Harmonic spectrum of input phase current,  $i_s$ .
- Fig. 7.1 Circuit Configuration of Cuk converter and isolated FB converter based AWPS.
- Fig. 7.2 Circuit Configuration of SEPIC and isolated FB converter based AWPS.
- Fig. 7.3 Circuit Configuration of zeta converter and isolated FB converter based AWPS.
- Fig. 7.4 Circuit Configuration of CSC converter and isolated FB converter based AWPS.
- Fig. 7.5 Circuit Configuration of I-CSC converter and isolated FB converter based AWPS.
- Fig. 7.6 Operating modes of Cuk converter during steady state for the duration of one switching cycle (a) Mode I; (b) Mode II; (c) Mode III; (d) Waveforms during one switching period.
- Fig. 7.7 Operating modes of SEPIC during steady state for the duration of one switching cycle (a) Mode I; (b) Mode II; (c) Mode III; (d) Waveforms during one switching period.
- Fig. 7.8 Operating modes of zeta converter during steady state for the duration of one switching cycle; (a) Mode I; (b) Mode II; (c) Mode III; (d) Waveforms during one switching period.
- Fig. 7.9 Operation of CSC converter for the duration of one switching cycle (a) Mode-I, (b) Mode-II, (c) Mode-III, (d) Waveforms during one switching period.
- Fig. 7.10 Operating modes of interleaved CSC converter during one switching period (a-f); (a) Mode-I; (b) Mode-II; (c) Mode-III; (d) Mode-IV; (e) Mode-V; (f) Mode-VI; (g) Waveforms during one switching period.
- Fig. 7.11 MATLAB model of Cuk converter based two-stage AWPS.
- Fig. 7.12 MATLAB model of non-isolated SEPIC based AWPS.
- Fig. 7.13 MATLAB model of non-isolated zeta converter based AWPS.
- Fig. 7.14 MATLAB model of CSC converter based AWPS.

- Fig. 7.15 MATLAB model of interleaved-CSC converter based SMPS.
- Fig. 7.16 Experimental developed hardware of CSC converter based SMPS for arc welding.
- Fig. 7.17 Experimental prototype of interleaved-CSC converter based SMPS for arc welding.
- Fig. 7.18 Measured PQ indices of conventional AWPS at rated load with supply voltage at 220V. (a) Conventional AWPS input voltage and current; (b) Input power and PF; (c) Harmonic spectrum of input current.
- Fig. 7.19 Performance of Cuk converter based AWPS at full load.
- Fig. 7.20 Waveform of input current and its harmonic spectrum at rated load.
- Fig. 7.21 Performance of Cuk converter based AWPS during light load condition.
- Fig. 7.22 Waveform of input current and its harmonic spectrum at light load.
- Fig. 7.23 Performance of Cuk converter based AWPS during overload condition.
- Fig. 7.24 Steady state performance of SEPIC based AWPS at full load.
- Fig. 7.25 Waveform of the input current and its harmonic spectrum at rated load.
- Fig. 7.26 Performance of SEPIC based AWPS during light load condition.
- Fig. 7.27 Waveform of input current and its harmonic spectrum during light load.
- Fig. 7.28 Dynamic performance of SEPIC based AWPS during overload condition.
- Fig. 7.29 Performance of zeta converter based AWPS at full load.
- Fig. 7.30 Waveform of input current and its harmonic spectrum at rated load.
- Fig. 7.31 Dynamic performance of zeta converter based AWPS during light load condition.
- Fig. 7.32 Waveform of input current and its harmonic spectrum during light load.
- Fig. 7.33 Dynamic performance of zeta converter based AWPS during overload condition.
- Fig. 7.34 Performance of CSC converter based AWPS at full load.
- Fig. 7.35 Waveform of input current and its harmonic spectrum at rated load.
- Fig. 7.36 Dynamic performance of CSC converter based AWPS during light load condition.
- Fig. 7.37 Waveform of input current and its harmonic spectrum at light load.
- Fig. 7.38 Performance of CSC converter based AWPS during overload condition.
- Fig. 7.39 Performance of interleaved CSC converter based AWPS at full load.
- Fig. 7.40 Waveform of input current and its harmonic spectrum at rated load.
- Fig. 7.41 Dynamic performance of interleaved-CSC converter based AWPS during light load condition.
- Fig. 7.42 Waveform of input current and its harmonic spectrum during light load.

- Fig. 7.43 Dynamic performance of interleaved-CSC converter based AWPS during overload condition.
- Fig. 7.44 Input voltage, input current and output voltage and current of FB DC-DC converter.
- Fig. 7.45 Input voltage, input current and output voltage and current of CSC converter.
- Fig. 7.46 Input voltage, intermediate capacitor voltage and inductor current of CSC converter.
- Fig. 7.47 Input voltage, voltage and current stress of switch  $S_b$  intermediate capacitor voltage and inductor current of CSC converter.
- Fig. 7.48 PQ indices and performance parameters of the CSC converter based AWPS at rated load; (a) Input voltage and current; (b) Input power, PF and DPF; (c) Harmonic spectrum of input phase current,  $i_s$ .
- Fig. 7.49 Input voltage, input current and output voltage and current of FB DC-DC converter during light load condition.
- Fig. 7.50 PQ indices and performance parameters of the interleaved CSC converter based AWPS during light load; (a) Input voltage and current; (b) Input power, PF and DPF; (c) Harmonic spectrum of input phase current,  $i_s$ .
- Fig. 7.51 Input voltage, input current and output voltage and current of FB DC-DC converter during overload condition.
- Fig. 7.52 Input voltage, input current and output voltage and current of FB DC-DC converter.
- Fig. 7.53 Input voltage, input current and output voltage and current of interleaved CSC converter.
- Fig. 7.54 Input voltage, intermediate capacitor voltage and inductor current of interleaved CSC converter.
- Fig. 7.55 Input voltage, voltage and current stress of switch  $S_{b1}$  intermediate capacitor voltage and inductor current of interleaved CSC converter.
- Fig. 7.56 PQ indices and performance parameters of the interleaved CSC converter based AWPS at rated load; (a) Input voltage and current; (b) Input power, PF and DPF; (c) Harmonic spectrum of input phase current,  $i_s$ .
- Fig. 7.57 Input voltage, input current and output voltage and current of FB DC-DC converter during light load condition.
- Fig. 7.58 PQ indices and performance parameters of the interleaved CSC converter based AWPS during light load; (a) Input voltage and current; (b) Input power, PF and DPF; (c) Harmonic spectrum of input phase current,  $i_s$ .

- Fig. 7.59 Input voltage, input current and output voltage and current of FB DC-DC converter during overload condition.
- Fig. 8.1 Basic configuration of single phase two-stage SMPS.
- Fig. 8.2 Circuit configuration of the BL-Cuk converter based AWPS.
- Fig. 8.3 BL Cuk converter during (a) positive and (b) negative half-cycles of the supply voltage.
- Fig. 8.4 Circuit configuration of the BL-SEPIC based AWPS.
- Fig. 8.5 Operating circuits of BL SEPIC during (a) positive and (b) negative half-cycles of the supply voltage.
- Fig. 8.6 Circuit configuration of the BL-zeta converter based AWPS.
- Fig. 8.7 BL-zeta converter during (a) positive and (b) negative half-cycles of the supply voltage.
- Fig. 8.8 Circuit configuration of the BL- CSC converter based AWPS.
- Fig. 8.9 BL-CSC converter during (a) positive and (b) negative half-cycles of the supply voltage.
- Fig. 8.10 Operating modes of BL-Cuk converter during steady state for the period of one switching cycle.
- Fig. 8.11 Operating modes of BL SEPIC during steady state for the period of one switching cycle.
- Fig. 8.12 Operating modes of BL-zeta converter during steady state for the period of one switching cycle.
- Fig. 8.13 Operating modes of BL-CSC converter during steady state for the period of one switching cycle.
- Fig. 8.14 MATLAB model of BL-Cuk converter based AWPS.
- Fig. 8.15 MATLAB model of BL-SEPIC based AWPS.
- Fig. 8.16 MATLAB model of BL-zeta converter based AWPS.
- Fig. 8.17 MATLAB model of BL-CSC converter based AWPS.
- Fig. 8.18 Experimental setup of developed hardware of the BL-zeta converter based SMPS for arc welding.
- Fig. 8.19 Experimental setup of developed hardware of the BL-CSC converter based SMPS for arc welding.
- Fig. 8.20 Measured PQ indices of conventional AWPS at rated load with supply voltage at 220V. (a) Conventional AWPS input voltage and current; (b) Input power and PF; (c) Harmonic spectrum of input current.

- Fig. 8.21 Performance of BL-Cuk converter based AWPS at full load.
- Fig. 8.22 Waveform of input current and its harmonic spectrum at rated load.
- Fig. 8.23 Performance of BL-Cuk converter based AWPS during light load condition.
- Fig. 8.24 Waveform of input current and its harmonic spectrum at light load.
- Fig. 8.25 Performance of BL-Cuk converter based AWPS during overload condition.
- Fig. 8.26 Performance of BL-SEPIC based AWPS at full load.
- Fig. 8.27 Waveform of input current and its harmonic spectrum at rated load.
- Fig. 8.28 Dynamic performance of BL-SEPIC based AWPS during light load condition.
- Fig. 8.29 Waveform of input current and its harmonic spectrum during light load.
- Fig. 8.30 Performance of BL-SEPIC based AWPS during overload condition.
- Fig. 8.31 Performance of BL-zeta converter based AWPS at full load.
- Fig. 8.32 Waveform of input current and its harmonic spectrum at rated load.
- Fig. 8.33 Performance of BL-zeta converter based AWPS during light load condition.
- Fig. 8.34 Waveform of input current and its harmonic spectrum during light load.
- Fig. 8.35 Performance of BL-zeta converter based AWPS during overload condition.
- Fig. 8.36 Performance of BL-CSC converter based AWPS at full load.
- Fig. 8.37 Waveform of input current and its harmonic spectrum at rated load.
- Fig. 8.38 Performance of BL-CSC converter based AWPS during light load condition.
- Fig. 8.39 Waveform of input current and its harmonic spectrum during light load.
- Fig. 8.40 Performance of BL-CSC converter based AWPS during overload condition.
- Fig. 8.41 Input voltage, input current and output voltage and current of FB DC-DC converter.
- Fig. 8.42 Input voltage, intermediate capacitor voltage, input inductor current and output inductor current of BL-zeta converter during positive half cycle of the input voltage.
- Fig. 8.43 Input voltage, voltage switch stress of the switch conducting in positive half cycle and voltage switch stress of the switch conducting in negative half cycle of the input voltage.
- Fig. 8.44 Input voltage, switch stress of the switch conducting in positive half cycle of the input voltage.
- Fig. 8.45 Enlarged waveforms of voltage and current stresses of switch conducting in positive half cycle of input voltage.

- Fig. 8.46 PQ indices and performance parameters of the BL-zeta converter based AWPS at rated load; (a) Input voltage and current; (b) Input power, PF and DPF; (c) Harmonic spectrum of input phase current,  $i_s$ .
- Fig. 8.47 Input voltage, input current and output voltage and current of FB DC-DC converter during light load condition.
- Fig. 8.48 PQ indices and performance parameters of the BL-Zeta converter based AWPS during light load; (a) Input voltage and current; (b) Input power, PF and DPF; (c) Harmonic spectrum of input phase current,  $i_s$ .
- Fig. 8.49 Input voltage, input current and output voltage and current of FB DC-DC converter during overload condition.
- Fig. 8.50 Input voltage, input current and output voltage and current of FB DC-DC converter.
- Fig. 8.51 Input voltage, voltage switch stress of the switch conducting in positive half cycle and voltage switch stress of the switch conducting in negative half cycle of the input voltage.
- Fig. 8.52 Input voltage, inductor current and intermediate capacitor voltage of BL-CSC converter during positive half cycle of the input voltage.
- Fig. 8.53 Input voltage, switch stress of the switch conducting in one half cycle of the input voltage.
- Fig. 8.54 Enlarged waveforms of voltage and current stresses of switch conducting in positive half cycle of input voltage.
- Fig. 8.55 PQ indices and performance parameters of the BL-CSC converter based AWPS at rated load; (a) input voltage and current; (b) Input power, PF and DPF; (c) Harmonic spectrum of input phase current,  $i_s$ .
- Fig. 8.56 Input voltage, input current and output voltage and current of FB DC-DC converter during light load condition.
- Fig. 8.57 PQ indices and performance parameters of the BL-CSC converter based AWPS during light load; (a) Input voltage and current; (b) Input power, PF and DPF; (c) Harmonic spectrum of input phase current,  $i_s$ .
- Fig. 8.58 Input voltage, input current and output voltage and current of FB DC-DC converter during overload condition.
- Fig. 9.1 Circuit configuration of the proposed VR based AWPS.
- Fig. 9.2 Eight different switching combinations tabulated in Table-9.1; denoted by the triple of the phase switching functions ( $S_a, S_b, S_c$ ). (a) (ON, ON, ON); (b) (ON, ON, OFF); (c) (ON, OFF, OFF); (d) (ON, OFF, ON); (e) (OFF, OFF, ON); (f) (OFF, ON, ON); (g) (OFF, ON, OFF); (h) (OFF, OFF, OFF).

- Fig. 9.3 Control scheme used for VR.
- Fig. 9.4 Simulation model of three phase VR based SMPS for arc welding application.
- Fig. 9.5 Developed hardware of proposed VR based SMPS.
- Fig. 9.6 Steady state performance of VR based AWPS using MATLAB/Simulink environment.
- Fig. 9.7 Waveform of input AC mains phase 'a' current ( $i_s$ ) along with its harmonic spectrum at 415V.
- Fig. 9.8 Dynamic performance of VR based AWPS during light conditions and at input voltage of 415V.
- Fig. 9.9 Waveform of input ac mains phase 'a' current ( $i_s$ ) along with its harmonic spectrum at 20% load.
- Fig. 9.10 Performance of VR based AWPS during short circuit condition.
- Fig. 9.11 Recorded waveforms of  $v_{ab}$ ,  $i_a$ ,  $V_o$  and  $I_o$  at rated load condition.
- Fig. 9.12 Recorded waveforms of  $v_{ab}$ ,  $i_a$ ,  $V_d$  and  $I_d$  at rated load condition.
- Fig. 9.13 Recorded waveforms of DC-link capacitors' voltage  $V_{C1}$  and  $V_{C2}$ .
- Fig. 9.14 Recorded waveforms of  $v_{ab}$ ,  $i_a$ ,  $V_{BA}$  and  $V_d$ .
- Fig. 9.15 Recorded waveforms of  $v_{ab}$ ,  $i_a$ ,  $i_b$  and  $i_c$ .
- Fig. 9.16 Recorded PQ indices of the proposed SMPS at rated load with line voltage as 230V; (a) Proposed SMPS input voltage and current; (b) Input power and DPF; (c) Harmonic spectrum of input phase current,  $i_a$ ; (d) Harmonic spectrum of input line voltage,  $v_{ab}$ .
- Fig. 9.17 Waveforms of  $v_{ab}$ ,  $i_a$ ,  $V_o$  and  $I_o$  under light load condition.
- Fig. 9.18 Recorded PQ indices of the proposed SMPS at light load with line voltage as 230V; (a) Proposed SMPS input voltage and current; (b) Input power and DPF; (c) Harmonic spectrum of input phase current,  $i_a$ ; (d) Harmonic spectrum of input line voltage,  $v_{ab}$ .
- Fig. 9.19 Waveforms of  $v_{ab}$ ,  $i_a$ ,  $V_o$  and  $I_o$  under overload condition.
- Fig. 10.1 Circuit configuration of 18-pulse AC-DC converter based AWPS.
- Fig. 10.2 Winding diagram of delta-polygon connected autotransformer based 18-pulse AC-DC converter.
- Fig. 10.3 Phasor diagram of delta-polygon connected autotransformer based 18-pulse AC-DC converter.
- Fig. 10.4 Winding currents between phase 'a' and 'b' for a delta polygon autoconnected transformer based 18-pulse AC-DC converter.

- Fig. 10.5 Input current  $i_a$  of three-phase DBR, winding currents ( $i_{ab1}$  and  $i_{ac1}$ ) and input line current ( $i_{sa}$ ) of a delta polygon autoconnected transformer based 18-pulse AC-DC converter.
- Fig. 10.6 Simulation model of three phase 18-pulse converter based SMPS for arc welding application.
- Fig. 10.7 System configuration of the developed laboratory prototype.
- Fig. 10.8 Developed hardware of proposed 18-pulse AC-DC converter based AWPS.
- Fig. 10.9 Steady state performance of the multipulse converter based AWPS in MATLAB/Simulink.
- Fig. 10.10 Waveform of input AC mains phase 'a' current ( $i_{sa}$ ) along with its harmonic spectrum at 415V.
- Fig. 10.11 Waveform of input AC mains phase 'a' current ( $i_{sa}$ ) and DBR currents-  $i_a$ ,  $i_{a1}$  and  $i_{a2}$ .
- Fig. 10.12 Waveforms of intermediate current components  $i_{ab1}$ ,  $i_{bc4}$ ,  $i_{ac5}$  and  $i_{ab3}$ .
- Fig. 10.13 Dynamic performance of multipulse converter based AWPS during light conditions.
- Fig. 10.14 Waveform of input AC mains phase 'a' current ( $i_s$ ) along with its harmonic spectrum at 20% load.
- Fig. 10.15 Performance of proposed AWPS during short circuit condition.
- Fig. 10.16 Recorded waveforms of  $v_{ab}$ ,  $i_a$ ,  $V_o$  and  $I_o$  at rated load condition.
- Fig. 10.17 Recorded PQ indices of the proposed AWPS at rated load with line voltage as 170V; (a) Proposed AWPS input voltage and current; (b) Input power and DPF; (c) Harmonic spectrum of input phase current,  $i_a$ ; (d) Harmonic spectrum of input line voltage,  $v_{ab}$ .
- Fig. 10.18 Input currents of DBRs to illustrate the phase-shifted operation of 18-pulse AC-DC converter.
- Fig. 10.19 Recorded waveforms input currents of DBRs (a) Waveform of current  $i_a$ , (b) Waveform of current  $i_{a1}$  and (c) Waveform of current  $i_{a2}$ .
- Fig. 10.20 Recorded waveforms winding currents (a) Waveform of current  $i_{ab1}$ , (b) Waveform of current  $i_{bc4}$ , (c) Waveform of current  $i_{ac5}$ , (d) Waveform of current  $i_{ab3}$ , (e) Waveform of current  $i_{ac1}$ .
- Fig. 10.21 Waveforms of  $v_{ab}$ ,  $i_a$ ,  $V_o$  and  $I_o$  under light load condition.
- Fig. 10.22 Recorded PQ indices of the proposed AWPS at light load with line voltage as 170V; (a) Proposed AWPS input voltage and current; (b) Input power and DPF; (c) Harmonic spectrum of input phase current,  $i_a$ ; (d) Harmonic spectrum of input line voltage,  $v_{ab}$ .

- Fig. 10.23 Waveforms of  $v_{ab}$ ,  $i_a$ ,  $V_o$  and  $I_o$  under overload condition.
- Fig. 11.1 Basic configuration of three-phase single-stage SMPS.
- Fig. 11.2 Basic configuration of three-phase single-stage BL-SMPS.
- Fig. 11.3 Schematic of a modular FB buck converter based AWPS.
- Fig. 11.4 Schematic of a modular push-pull converter based AWPS.
- Fig. 11.5 Schematic of modular isolated Cuk converter based AWPS.
- Fig. 11.6 Schematic of modular isolated zeta converter based AWPS.
- Fig. 11.7 Schematic of a BL-modular isolated Cuk converter based AWPS.
- Fig. 11.8 Circuit configuration of a BL-modular zeta converter based AWPS.
- Fig. 11.9 Operation of FB buck converter (a) Mode-I: switch  $S_1$  and  $S_4$  conducting, (b) Mode-II: both the switches are off, (c) Mode-III: Output Inductor in DCM, (d) Mode-IV: switch  $S_2$  and  $S_3$  are on, (e) Mode-V: both the switches are off, (c) Mode-VI: Output Inductor in DCM.
- Fig. 11.10 Operation of push-pull buck converter (a) Mode-I: switch  $S_1$  conducting, (b) Mode-II: both the switches are off, (c) Mode-III: Output Inductor in DCM, (d) Mode-IV: switch  $S_2$  is on, (e) Mode-V: both the switches are off, (c) Mode-VI: Output Inductor in DCM.
- Fig. 11.11 MATLAB model of FB modular converter based AWPS.
- Fig. 11.12 MATLAB model of push-pull modular converter based AWPS.
- Fig. 11.13 MATLAB model of Cuk modular converter based AWPS.
- Fig. 11.14 MATLAB model of zeta modular converter based AWPS.
- Fig. 11.15 MATLAB model of BL-Cuk modular converter based AWPS.
- Fig. 11.16 MATLAB model of BL-zeta converter based modular AWPS.
- Fig. 11.17 Performance of FB modular converter based AWPS at full load.
- Fig. 11.18 Waveform of input current ( $i_{sa}$ ) and its harmonic spectrum at rated load.
- Fig. 11.19 Dynamic performance of FB modular converter based AWPS during light load condition.
- Fig. 11.20 Waveform of input current and its harmonic spectrum at light load.
- Fig. 11.21 Performance of FB modular converter based AWPS during overload condition.
- Fig. 11.22 Performance of push-pull modular converter based AWPS at full load.
- Fig. 11.23 Waveform of input current ( $i_{sa}$ ) and its harmonic spectrum at rated load.
- Fig. 11.24 Dynamic performance of push-pull modular converter based AWPS during light load condition.

- Fig. 11.25      Waveform of the input current and its harmonic spectrum at light load.
- Fig. 11.26      Performance of push-pull modular converter based AWPS during overload condition.
- Fig. 11.27      Performance of isolated Cuk modular converter based AWPS at full load.
- Fig. 11.28      Waveform of input current ( $i_{sa}$ ) and its harmonic spectrum at rated load.
- Fig. 11.29      Dynamic performance of isolated Cuk modular converter based AWPS during light load condition.
- Fig. 11.30.     Waveform of input current and its harmonic spectrum at light load.
- Fig. 11.31      Performance of isolated Cuk modular converter based AWPS during overload condition.
- Fig. 11.32      Performance of isolated zeta modular converter based AWPS at full load.
- Fig. 11.33      Waveform of input current ( $i_{sa}$ ) and its harmonic spectrum at rated load.
- Fig. 11.34      Dynamic performance of isolated zeta modular converter based AWPS during light load condition.
- Fig. 11.35      Waveform of input current and its harmonic spectrum at light load.
- Fig. 11.36      Performance of isolated zeta modular converter based AWPS during overload condition.
- Fig. 11.37      Performance of isolated BL-Cuk modular converter based AWPS at full load.
- Fig. 11.38      Waveform of input current ( $i_{sa}$ ) and its harmonic spectrum at rated load.
- Fig. 11.39      Dynamic performance of isolated BL-Cuk modular converter based AWPS during light load condition.
- Fig. 11.40.     Waveform of input current and its harmonic spectrum at light load.
- Fig. 11.41      Performance of isolated BL-Cuk modular converter based AWPS during overload condition.
- Fig. 11.42      Performance of isolated BL-zeta modular converter based AWPS at full load.
- Fig. 11.43      Waveform of input current ( $i_{sa}$ ) and its harmonic spectrum at rated load.
- Fig. 11.44      Dynamic performance of isolated BL-zeta modular converter based AWPS during light load condition.
- Fig. 11.45      Waveform of input current and its harmonic spectrum at light load.
- Fig. 11.46      Performance of isolated BL-zeta modular converter based AWPS during overload condition.

## **LIST OF TABLES**

Table 4.1	Design specifications for TS zeta converter based AWPS
Table 4.2	Design specifications for Sheppard Taylor converter based AWPS
Table 4.3	Design specifications for TS Zeta Converter Based AWPS
Table 5.1	Design specifications for BL-FB converter based AWPS
Table 5.2	Design specifications for isolated BL-Cuk converter based AWPS
Table 5.3	Design specifications for isolated BL-SEPIC based AWPS
Table 5.4	Design specifications for isolated BL-zeta converter Based AWPS
Table 5.5	Design specifications for isolated BL-zeta converter Based AWPS
Table 6.1	Design specifications for boost converter based AWPS
Table 6.2	Design specifications for interleaved boost converter based AWPS
Table 6.3	Design specifications for bridgeless boost converter based AWPS
Table 7.1	Different modes for interleaved CSC converter based AWPS
Table 7.2	Design specifications for Cuk converter based AWPS
Table 7.3	Design specifications for SEPIC based AWPS
Table 7.4	Design specifications for zeta converter based AWPS
Table 7.5	Design specifications for CSC converter based AWPS
Table 7.6	Design specifications for interleaved CSC converter based AWPS
Table 7.7	Specifications for CSC converter based AWPS
Table 7.8	Specifications for interleaved CSC converter based AWPS
Table 8.1	Design specifications For BL-Cuk converter based AWPS
Table 8.2	Design specifications for BL-SEPIC based AWPS
Table 8.3	Design specifications for BL-zeta converter based AWPS

Table 8.4	Design specifications for BL-CSC converter based AWPS
Table 8.5	Specifications for BL-zeta converter based AWPS
Table 8.6	Specifications for BL-CSC converter based AWPS
Table 9.1	Eight different switching combinations
Table 9.2	Specifications for VR based AWPS
Table 10.1	Design specifications for multipulse converter based AWPS
Table 10.2	Design specifications of transformers used in 18-pulse converter
Table 10.3	Design specifications for multipulse converter based AWPS
Table 11.1	Design specifications for FB converter based modular AWPS
Table 11.2	Design specifications for push-pull converter based modular AWPS
Table 11.3	Design specifications for Cuk converter based modular AWPS
Table 11.4	Design specifications for zeta converter based modular AWPS
Table 11.5	Design specifications for BL-Cuk converter based modular AWPS
Table 11.6	Design specifications for BL-zeta converter based modular AWPS

## LIST OF ABBREVIATIONS/SYMBOLS

AWPS	Arc Welding Power Supply
BL	Bridgeless
CCM	Continuous Conduction Mode
CF	Crest Factor
CSC	Canonical Switching Cell
DBR	Diode Bridge Rectifier
DCM	Discontinuous Conduction Mode
DF	Distortion Factor
DICM	Discontinuous Inductor Current Mode
DPF	Displacement Power Factor
DSP	Digital Signal Processor
FB	Full Bridge
HFT	High Frequency Transformer
IEC	International Electrotechnical Commission
PCC	Point of Common Coupling
PF	Power Factor
PFC	Power Factor Correction
PI	Proportional Integral
PQ	Power Quality
PWM	Pulse Width Modulation
SEPIC	Single Ended Primary Inductance Converter
SMPS	Switched Mode Power Supply
SPS	Sim Power System
THD	Total Harmonic Distortion
$C_f$	Input Filter Capacitor (F)
$C_o$	Output Filter Capacitor (F)
$D$	Duty Ratio
$f_b$	Switching Frequency of Non-Isolated Front-End Converter (Hz)

$f_s$	Switching Frequency of Isolated Converter (Hz)
$\Delta I_o$	Ripple Current (A)
$I_b$	Output Current of First Stage (A)
$I_o$	Output Current (A)
$i_s$	Supply Current (A)
$i_{sa}, i_{sb}, i_{sc}$	Supply Currents in Three-Phase System (A)
$k_{pi}, k_{ii}, k'_{pi}, k'_{ii}$	Proportional and Integral Gains of Current Controllers
$k_{pv}, k_{iv}, k'_{pv}, k'_{iv}$	Proportional and Integral Gains of Voltage Controllers
$L_f$	Input Filter Inductor (H)
$L_m$	Magnetizing Inductance of HFT (H)
$L_o$	Output Filter Inductor (H)
$n$	HFT Turns Ratio
$N_1$	Number of Turns of Primary Winding of HFT
$N_2$	Number of Turns of Secondary Winding of HFT
$P_{in}$	Input Power (W)
$P_o$	Output Power (W)
$R_o$	Resistive Load at the Output ( $\Omega$ )
$\Delta V_o$	Ripple Voltage (V)
$V_b$	Output Voltage of First Stage (V)
$v_{L-L}$	Line-to-Line Voltage (V)
$V_o$	Output Voltage (V)
$v_s$	Supply Voltage (V)
$v_{sa}, v_{sb}, v_{sc}$	Supply Voltages in Three-Phase System (V)